Available online at www.sciencedirect.com
SCIENCE DIRECT®
PERGAMON
International Journal of Heat and Mass Transfer 46 (2003) 3927–3934
International Journal of HEAT and MASS TRANSFER
www.elsevier.com/locate/ijhmt

# Linear analysis of an aerothermal instability occurring in diffusion-controlled premixed catalytic combustion

Gérard Capitaine *

*Chemin de Pierre-Grise 13, CH-1294 Genthod/Geneva, Switzerland*

Received 12 June 2002

**Abstract**

The onset of the unstable temperature distribution which may appear in plane axisymmetric catalytic burner is studied. The instability mechanism is assumed to be related with the temperature dependence of the viscosity, thus with the pressure drop in the porous combustor, governed by Darcy's law. An area e.g., of lower temperature (dark zone) characterised by a smaller value of the kinetic viscosity gives rise to a locally increased gas flow mass velocity, the pressure drop remaining constant over the burner cross-section. The locally increased mass velocity produces an enhanced cooling of the area, whereby heat conduction from the hotter surrounding area tends to restore a homogeneous temperature distribution. A linear analysis of this thermal instability mechanism is carried out and yields a simple analytic solution for the state of neutral stability.


*Keywords:* Catalytic combustion; Thermal instability

## 1. Introduction

Experiments with a flat axisymmetric catalytic combustor operating with methane/air-mixtures at temperatures between 1000 and 1300 K showed a spatio-temporal unstable behaviour of the surface temperature distribution [1]. A sketch of the burner is shown in Fig. 1. The combustion gas and the air are premixed and evenly distributed over an insulating fibre-mat (layer I), followed by a permeable metallic foam structure (layer II), which is impregnated with a noble metal catalyst.

During combustion, transients may occur, during which at the catalytic surface spotwise dark zones appear (Fig. 2). Local temperature increase were also measured but "hot spots" could not be observed. In a case of a temperature rise, the burner is automatically shut off in order to prevent the catalytic panel from being damaged. The position and the extent of the dark zones were not repeatable, what indicates that their occurrence is not related with e.g., a local deactivation of the catalyst. It is notable that such dark zones do not vanish in time by heat conduction from the hotter, surrounding area. The occurrence of the dark zones depends on dimensional characteristics of the catalytic panel. These phenomena were observed with a catalytic panel of radius 70 mm (Fig. 2), but did not occur with a panel of radius 50 mm.

The appearance of the temperature inhomogeneity is also related with an unstable behaviour of the combustor itself. In the presence of dark spots, a small modification of the power or of the excess air ratio may e.g., lead to a sharp increase of the temperature, or also to a blowout of the burner. The dark zones arise and grow very slowly. However the difficult control of the burner (in the presence of dark spots) prevented from observing if the spots ever attained a steady state. The observed unstable burner behaviour seems to be the consequence and not the origin of a modification of the combustion parameters upon a burner having an inhomogeneous surface temperature distribution. The goal of the present investigation is to analyse and explain a possible thermal instability mode of plane axisymmetric catalytic panels and to determine the onset of such unstable combustion behaviour. This instability is supposed to exist, apart

* Tel.: +41-22-774-2243; fax: +41-22-774-2812.
*E-mail address:* gcapitaine@swissonline.ch (G. Capitaine).

0017-9310/03/$ - see front matter 
doi:10.1016/S0017-9310(03)00219-9

**Nomenclature**

*Notations*

| | |
|---|---|
| $a$ | specific surface area ($m^{-1}$) |
| $c_p$ | specific heat capacity of the gas ($J\,kg^{-1}\,K^{-1}$) |
| $c_s$ | specific heat capacity of the solid ($J\,kg^{-1}\,K^{-1}$) |
| $G$ | mass flow rate per unit area (mass velocity) ($kg\,s^{-1}\,m^{-2}$) |
| $g$ | mass velocity disturbance ($kg\,s^{-1}\,m^{-2}$) |
| $\Delta H_m$ | reaction enthalpy per unit mass ($J\,kg^{-1}$) |
| $K$ | permeability of the porous solid ($m^2$) |
| $k_r$ | radial thermal conductivity of the porous medium ($J\,m^{-1}\,s^{-1}\,K^{-1}$) |
| $k_z$ | axial thermal conductivity of the porous medium ($J\,m^{-1}\,s^{-1}\,K^{-1}$) |
| $L$ | length of the catalytic panel (m) |
| $n$ | temperature dependence exponent of the kinematic viscosity |
| $p$ | pressure (Pa) (not to confuse with the constant $p$ defined in (24)) |
| $r$ | radial space co-ordinate (m) |
| $R$ | radius of the catalytic panel (m) |
| $t$ | time (s) |
| $T$ | temperature (K) |
| $u$ | interstitial velocity ($m\,s^{-1}$) |
| $X$ | mass fraction of the lean reacting species (-) |
| $x$ | mass fraction disturbance (-) |
| $z$ | axial space co-ordinate (m) |
| $z_u$ | mass transfer unit length (m) |

*Greek symbols*

| | |
|---|---|
| $\beta$ | mass transfer coefficient ($m\,s^{-1}$) |
| $\varepsilon$ | void fraction (-) |
| $\vartheta$ | temperature disturbance (K) |
| $\nu$ | kinematic viscosity ($m^2\,s^{-1}$) |
| $\rho$ | density ($kg\,m^{-3}$) |

*Subscript*

| | |
|---|---|
| i | inlet |

*Dimensionless variables*

| | |
|---|---|
| $H$ | $X_i(-\Delta H_m)/c_pT_i$ |
| $Pe_r$ | $Gc_pR/k_r$ $Pe_{r,u,z}$ Péclet numbers for heat transfer |
| $Pe_u$ | $Gc_pz_u/k_z$ |
| $Pe_z$ | $Gc_pL/k_z$ |
| $T^*$ | $T/T_i$ |
| $X^*$ | $X/X_i$ |
| $x^*$ | $x/X_i$ |
| $\gamma$ | $g/G$ |
| $\varsigma$ | $z/L$ |
| $\varsigma_u$ | $z_u/L$ |
| $\eta$ | $r/R$ |
| $\vartheta^*$ | $\vartheta/T_i$ |
| $\mu$ | $\varepsilon\bar{\rho}c_p/[(1-\varepsilon)\rho_sc_s+\varepsilon\bar{\rho}c_p]$ |
| $\sigma$ | $L/R$ |
| $\tau$ | $Gt/\bar{\rho}\varepsilon L$ |

from the chemical kinetic instability effects which are discussed in the literature [2,3].

## 2. Analysis

### 2.1. Problem description and assumptions

The flow of fluids through porous media is generally governed by Poiseuille's law and Darcy's law [4]. In both cases, the pressure drop across the porous structure (combustor) is proportional to the kinematic viscosity. We assume the observed instability to be related with the temperature dependence of the kinematic viscosity. An area of lower temperature (dark zone) characterised by a smaller value of the kinematic viscosity gives rise to a locally increased gas flow mass velocity, the pressure drop remaining constant over the catalyst cross-section. The locally increased mass velocity produces an enhanced cooling of the area, whereby heat conduction from the hotter surrounding area tends to restore a homogeneous temperature distribution. The analysis of the behaviour of a plane axisymmetric adiabatic catalytic burner, which is subject to small disturbances of the gas mixture mass velocity profile is based on the following assumptions:

1. The temperatures of gas and solid at a given location are equal. This is a reasonable approximation for burners with a specific power below about $100\,kW/m^2$.
2. The heterogeneous catalytic reaction is limited by mass transfer. The burner was operating at temperatures from 1000 to 1300 K as the unstable behaviour occurred. Only the bulk concentration of the lean reactant is considered.
3. Due to the foam structure, axial as well as radial dispersion of the lean reacting species may be neglected. The experimentally determined mixing length is shown to be close to the foam pore diameter [5]. The Péclet numbers for axial and radial mass transport are respectively about 2 and 8 at pore diameter based Reynolds number $Re > 20$ [6]. Calculation with the estimated dispersion coefficients showed no influence on the limit of neutral stability.

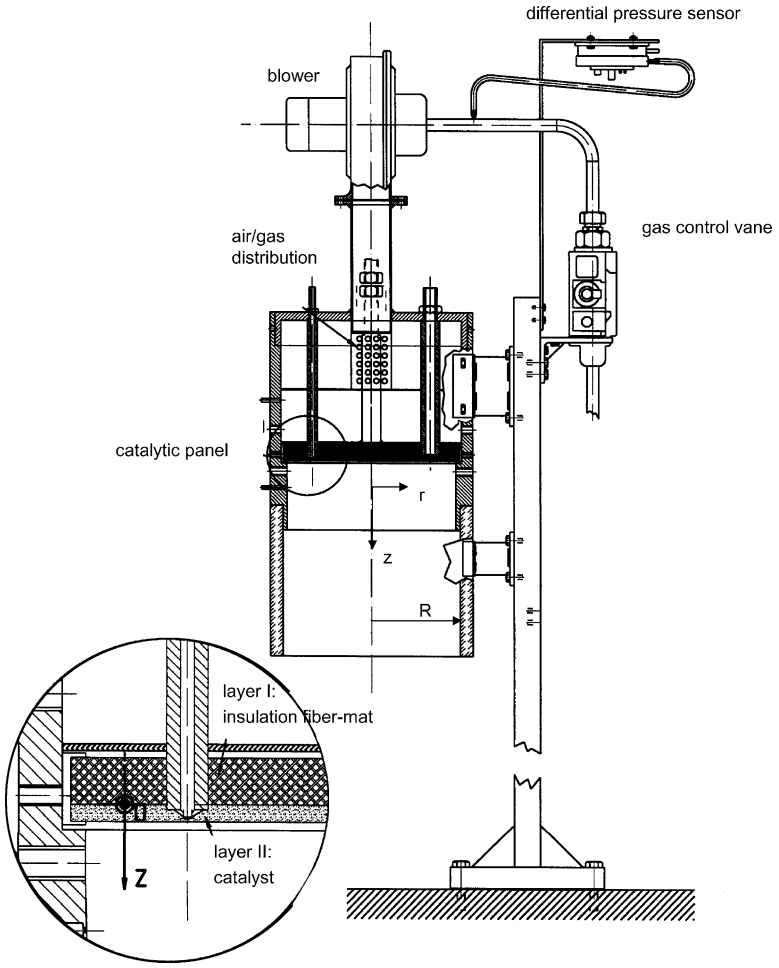


Fig. 1. Schematic figure of the combustor test bench. $R = 50$ and 70 mm. Thickness of the catalytic active layer II: 11 mm.

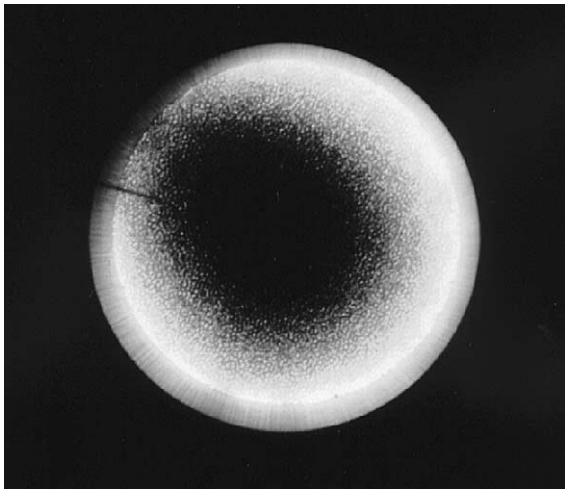

Fig. 2. Photograph of a dark zone at the surface of the catalytic panel. Radius of the catalytic panel: 70 mm.

4. The heat conduction within the gas–solid system is characterised by the axial and radial constant thermal conductivity, $k_z$ and $k_r$, respectively.
5. The radiative heat transfer is neglected. Its influence on the relative anisotropy of the thermal conductivity could not be established. Existing data are related to room-temperature measurements [7].
6. The radial combustor wall is adiabatic.
7. Once dark zones were visible, the observed variations of the temperature between the hotter and the colder (dark) zones at the surface of the catalytic panel were about 120 K, i.e. 10% of the operating temperature. In the linear stability analysis, much smaller temperature increments were supposed. Taking into account the operating temperature of the burner, the coefficient of volume expansion of gases is less than $10^{-3}$ $K^{-1}$. The variability in the density $\bar{\rho}$ due to the variations of temperature not exceeding 10 K (say) are at most 1% and may be neglected according to the Boussinesq approximation [8].

8. The combustion takes place at constant absolute pressure: $p_0 = \text{const}$.
9. The pressure drop across the porous structure of the burner ($\Delta p/p_0 \ll 1$) depends linearly on velocity according to Darcy's law. This behaviour was confirmed for the entire explored velocity range by pressure drop measurements.
10. The pressure drop is assumed steady and constant over the surface of the catalytic panel ($\partial \Delta p/\partial r = 0$) This assumption is generally valid only for an array of parallel ducts (honeycomb structures). For the sake of simplicity, this is supposed to apply in first approximation also to foams.
11. The velocity disturbances are assumed as axisymmetric profiles.

### 2.2. The basic equations

The equations governing the transport of momentum, energy and mass in a homogeneous model of a fixed bed are [4,6]

(a) *The equation of continuity*

$$\frac{\partial}{\partial z}(\tilde{\rho}\varepsilon\tilde{u}) = 0 \tag{1}$$

(b) *The equation of motion (Darcy's law)*

$$\tilde{\rho}\varepsilon\tilde{u} = -\frac{K}{\tilde{\nu}}\frac{\partial p}{\partial z} \tag{2}$$

(c) *The equation of heat transport*

$$\begin{aligned}[(1-\varepsilon)\rho_s c_s + \varepsilon\tilde{\rho}c_p]\frac{\partial \widetilde{T}}{\partial t} &= k_r\left(\frac{\partial^2 \widetilde{T}}{\partial r^2} + \frac{1}{r}\frac{\partial \widetilde{T}}{\partial r}\right) \\ &\quad + k_z\frac{\partial^2 \widetilde{T}}{\partial z^2} - \tilde{\rho}c_p\varepsilon\tilde{u}\frac{\partial \widetilde{T}}{\partial z} \\ &\quad + \tilde{\rho}a(-\Delta H_m)\beta\widetilde{X}\end{aligned} \tag{3}$$

(d) *The equation of mass transport*

$$\tilde{\rho}\varepsilon\frac{\partial \widetilde{X}}{\partial t} = -\tilde{\rho}\varepsilon\tilde{u}\frac{\partial \widetilde{X}}{\partial z} - \tilde{\rho}a\beta\widetilde{X} \tag{4}$$

(e) *The equation of state* ($p_0 = \text{const}$)

$$\frac{\tilde{\rho}}{\rho_i} = \frac{T_i}{\widetilde{T}} \tag{5}$$

(f) *The temperature dependence of the kinematic viscosity*

$$\frac{\tilde{\nu}}{\nu_i} = \left(\frac{\widetilde{T}}{T_i}\right)^n \tag{6}$$

The integration of Eqs. (1) and (2) with respect to $z$ make them more convenient for further development. The integration of Eq. (1) yields

$$\tilde{\rho}\varepsilon\tilde{u} = \widetilde{G}(r,t) \tag{7}$$

Introducing (7) into (2), we obtain by integration

$$\Delta p = -\frac{1}{K}\int_0^L \widetilde{G}(r,t)\tilde{\nu}(r,z,t)\mathrm{d}z \tag{8}$$

where, according to assumption (10), the pressure drop $\Delta p$ across the porous structure is steady and constant.

### 2.3. The perturbation equations

Assuming that the different variables describing the flow are subject to small disturbances with respect to their steady state values, we may write

$$\begin{aligned}\tilde{\rho} &= \bar{\rho}(z) + \rho(r,z,t) \\ \tilde{\nu} &= \bar{\nu}(z) + \nu(r,z,t) \\ \tilde{u} &= \bar{u}(z) + u(r,z,t) \\ \widetilde{T} &= T(z) + \vartheta(r,z,t) \\ \widetilde{X} &= X(z) + x(r,z,t) \\ \widetilde{G} &= G + g(r,t)\end{aligned} \tag{9}$$

where $\bar{\rho}(z)$, $\bar{\nu}(z)$, $\bar{u}(z)$, $T(z)$ and $X(z)$ are the radially uniform steady state solutions of Eqs. (1)–(6), $G$ the constant steady state mass velocity and

$$g(r,t) = \bar{\rho}u\varepsilon$$

the mass velocity disturbance.

Introducing the set (9) into the Eqs. (3)–(8) and neglecting all products and powers (higher than the first) of the disturbances $\rho$, $\nu$, $u$, $g$, $\vartheta$ and $x$, we obtain the set of linearized equations

$$\int_0^R g(r,t)r\,\mathrm{d}r = 0 \tag{10}$$

$$\frac{g}{G} = -\frac{\int_0^L \nu(r,z,t)\mathrm{d}z}{\int_0^L \bar{\nu}(z)\mathrm{d}z} \tag{11}$$

$$\begin{aligned}[(1-\varepsilon)\rho_s c_s + \varepsilon\bar{\rho}c_p]\frac{\partial \vartheta}{\partial t} &= k_r\left(\frac{\partial^2 \vartheta}{\partial r^2} + \frac{1}{r}\frac{\partial \vartheta}{\partial r}\right) \\ &\quad + k_z\frac{\partial^2 \vartheta}{\partial z^2} - Gc_p\frac{\partial \vartheta}{\partial z} - gc_p\frac{\partial T}{\partial z} \\ &\quad + \bar{\rho}a(-\Delta H_m)\beta x\end{aligned} \tag{12}$$

$$\bar{\rho}\varepsilon\frac{\partial x}{\partial t} = -G\frac{\partial x}{\partial z} - g\frac{\partial X}{\partial z} - \bar{\rho}a\beta x \tag{13}$$

Eq. (10) expresses the conservation of the total mass flow through the burner section and (11) is derived from (8) with the additional condition $\partial p/\partial r = 0$ over the catalytic panel.

The linearization of Eq. (6) leads to

$$\nu(r,z,t) = \bar{\nu}(z)n\frac{\vartheta(r,z,t)}{T(z)} \tag{14}$$

Introducing (14) into (11) gives

$$\frac{g}{G} = -n\frac{\int_0^L \bar{v}\frac{\vartheta}{T}\,\mathrm{d}z}{\int_0^L \bar{v}\,\mathrm{d}z}$$

or as a first approximation

$$\frac{g(r,t)}{G} \cong -\frac{n}{L}\int_0^L \frac{\vartheta(r,z,t)}{T(z)}\,\mathrm{d}z \tag{15}$$

In the perturbation equations (12) and (13), the axial gradients of the steady state temperature $T(z)$ and of the mass fraction $X(z)$ appear as the convective terms $g\partial T/\partial z$ and $g\partial X/\partial z$. $T(z)$ and $X(z)$ are obtained by means of Eqs. (3) and (4), where $\partial/\partial t = \partial/\partial r = 0$ i.e.

$$\frac{k_z}{Gc_p}\frac{\mathrm{d}^2T}{\mathrm{d}z^2} - \frac{\mathrm{d}T}{\mathrm{d}z} + \frac{\bar{\rho}a\beta}{G}\frac{(-\Delta H_m)}{c_p}X = 0 \tag{16}$$

$$\frac{\mathrm{d}X}{\mathrm{d}z} + \frac{\bar{\rho}a\beta}{G}X = 0 \tag{17}$$

with the boundary conditions

$$z = 0 \quad Gc_p(T_i - T) = -k_z\frac{\partial T}{\partial z}$$
$$z = L \quad \frac{\partial T}{\partial z} = 0$$
$$z = 0 \quad X = X_i$$

The boundary conditions of the energy equation state that (a) the convective heat flux equals the conductive heat flux at the "cold boundary" $z = 0$ and that (b) the temperature gradient at the "hot boundary" $z = L$ vanishes.

The expression $\bar{\rho}a\beta/G$ in (16) and (17) represents the inverse of the mass transfer unit length $z_u$ related to the diffusion-controlled catalytic combustion process [9]. In that case, the bulk concentration of the reactants will decay exponentially. The $e^{-1}$ decay represents one mass transfer unit and $z_u$ the corresponding length.

The integration of (16) and (17) yields

$$\frac{T}{T_i} = 1 + \frac{X_i(-\Delta H_m)}{c_pT_i}\left[\frac{1 + Pe_u[1 - \exp(-z/z_u)]}{1 + Pe_u}\right] \tag{18}$$

and

$$\frac{X}{X_i} = \exp(-z/z_u) \tag{19}$$

with

$$Pe_u \equiv \frac{Gc_pz_u}{k_z}$$

a Péclet number based on $z_u$.

Replacing $g$ in (12) and (13) by (15) and expressing Eqs. (12), (13), (18) and (19), with the defined non-dimensional variables, (the asterisk being dropped in order to make the writing easier), we obtain

$$\frac{1}{\mu}\frac{\partial\vartheta}{\partial\tau} - \frac{1}{Pe_r}\sigma\left(\frac{\partial^2\vartheta}{\partial\eta^2} + \frac{1}{\eta}\frac{\partial\vartheta}{\partial\eta}\right) - \frac{1}{Pe_z}\frac{\partial^2\vartheta}{\partial\varsigma^2} + \frac{\partial\vartheta}{\partial\varsigma} - \frac{H}{\varsigma_u}x - \frac{\partial T}{\partial\varsigma}n\int_0^1 \frac{\vartheta}{T}\,\mathrm{d}\varsigma = 0 \tag{20}$$

$$\frac{\partial x}{\partial\tau} + \frac{\partial x}{\partial\varsigma} + \frac{1}{\varsigma_u}x - \frac{\partial X}{\partial\varsigma}n\int_0^1 \frac{\vartheta}{T}\,\mathrm{d}\varsigma = 0 \tag{21}$$

$$T = 1 + H\frac{1 + Pe_u[1 - \exp(-\varsigma/\varsigma_u)]}{1 + Pe_u} \tag{22}$$

$$X = \exp(-\varsigma/\varsigma_u) \tag{23}$$

Despite of having neglected the radial reacting species dispersion in Eq. (21), the convective bulk mass transport still depends on the radial variation of the mass velocity.

### 2.4. Boundary conditions

The solutions of Eqs. (20) and (21) must satisfy boundary conditions which depend on the characteristics of the combustion process. These boundary conditions are set by the required axial symmetry, the thermal insulation of the combustor casing wall and the continuity of the heat flux in axial direction:

$$\eta = 0 \quad \frac{\partial\vartheta}{\partial\eta} = 0 \tag{24a}$$

$$\eta = 1 \quad \frac{\partial\vartheta}{\partial\eta} = 0 \tag{24b}$$

$$\varsigma = 0 \quad \vartheta + (1 - T)n\int_0^1 \frac{\vartheta}{T}\,\mathrm{d}\varsigma - \frac{1}{Pe_z}\frac{\partial\vartheta}{\partial\varsigma} = 0 \tag{24c}$$

$$\varsigma = 0 \quad x = 0 \tag{24d}$$

$$\varsigma = 1 \quad \frac{\partial\vartheta}{\partial\varsigma} = 0 \tag{24e}$$

### 2.5. Solution of the perturbation equations

The solutions of the Eqs. (20) and (21) can be written in form of a product of functions in $\tau$, $\eta$ and $\varsigma$

$$\vartheta = \mathrm{e}^{p\tau}\Gamma(\eta)Z(\varsigma)$$
$$x = \mathrm{e}^{p\tau}\Gamma(\eta)\chi(\varsigma) \tag{25}$$

where $p$ is a constant which can be complex.

By inserting (23) and (25) into Eq. (21), its solution with the boundary condition (24d) becomes

$$\chi = \frac{1}{p\varsigma_u}\left[\exp\left(-(p\varsigma_u + 1)\frac{\varsigma}{\varsigma_u}\right) - \exp\left(-\frac{\varsigma}{\varsigma_u}\right)\right]n \times \int_0^1 \frac{Z}{T}\,\mathrm{d}\varsigma \tag{26}$$

which may be written in abbreviated form

$$\chi = \varphi(p,\varsigma) n \int_0^1 \frac{Z}{T}\,\mathrm{d}\varsigma \tag{26a}$$

By inserting (25) and (26a) into Eq. (20), the partial differential equation is split into two ordinary differential equations, each for a single independent variable

$$\frac{\mathrm{d}^2\Gamma}{\mathrm{d}\eta^2} + \frac{1}{\eta}\frac{\mathrm{d}\Gamma}{\mathrm{d}\eta} + \lambda\Gamma = 0 \tag{27}$$

and

$$\frac{\mathrm{d}^2 Z}{\mathrm{d}\varsigma^2} - Pe_z\frac{\mathrm{d}Z}{\mathrm{d}\varsigma} - \left(Pe_z\frac{p}{\mu} + \frac{k_r}{k_z}\lambda\sigma^2\right)Z + Pe_z\left(\frac{H}{\varsigma_u}\varphi + \frac{\mathrm{d}T}{\mathrm{d}\varsigma}\right)n \times \int_0^1 \frac{Z}{T}\,\mathrm{d}\varsigma = 0 \tag{28}$$

with the separation constant $\lambda$.

The solution of Eq. (27) is

$$\Gamma = J_0(\sqrt{\lambda}\eta) \tag{29}$$

$J_0$ being the Bessel function of the first kind of order 0. Taking into account the radial boundary condition (24b) we obtain

$$\left(\frac{\mathrm{d}\Gamma}{\mathrm{d}\eta}\right)_{\eta=1} = -\sqrt{\lambda}J_1(\sqrt{\lambda}) = 0 \tag{30}$$

giving the allowable values of $\lambda$ as the zeros $j_{1,k}$ of the Bessel function $J_1$ ie.

$$\sqrt{\lambda_k} = j_{1,k} \quad k = 1,2,3,\ldots \tag{31a}$$

and the related allowed functions

$$\Gamma_k = J_0(j_{1,k}\eta) \quad k = 1,2,3,\ldots \tag{31b}$$

As is easily shown, condition (30) fulfils also the required condition (10), which in non-dimensional variables becomes

$$\int_0^1 \gamma\eta\,\mathrm{d}\eta = 0 \tag{32}$$

Inserting (15) into (32) and taking into account (25) and (29) yields

$$\int_0^1 \gamma\eta\,\mathrm{d}\eta = -n\int_0^1 \frac{Z}{T}\,\mathrm{d}\varsigma \int_0^1 J_0\left(\sqrt{\lambda_k}\eta\right)\eta\,\mathrm{d}\eta = 0$$

since

$$\int_0^1 J_0\left(\sqrt{\lambda_k}\eta\right)\eta\,\mathrm{d}\eta = \frac{1}{\sqrt{\lambda_k}}J_1\left(\sqrt{\lambda_k}\right)$$

and according to (31a) $\sqrt{\lambda_k}$ are the zeros of $J_1$.

According to classical methods, the solution of Eq. (28) is

$$Z_k = \hat{\boldsymbol{h}}_k + \hat{\boldsymbol{q}}_k \tag{33}$$

where

$$\hat{\boldsymbol{h}}_k = \hat{c}_{k1}\exp(s_{k1}\varsigma) + \hat{c}_{k2}\exp(s_{k2}\varsigma) \tag{33a}$$

is the general solution of the homogeneous equation and

$$\hat{\boldsymbol{q}}_k = -\frac{\alpha_k}{s_{k1}-s_{k2}}\left[\exp(s_{k1}\varsigma)\int \psi_k\exp(-s_{k1}\varsigma)\,\mathrm{d}\varsigma - \exp(s_{k2}\varsigma)\int \psi_k\exp(-s_{k2}\varsigma)\,\mathrm{d}\varsigma\right] \tag{33b}$$

is a solution of the inhomogeneous equation. The factors $\alpha_k$ and $\psi_k$ in (33b) are defined as

$$\alpha_k = n\int_0^1 \frac{Z_k}{T}\,\mathrm{d}\varsigma \tag{34}$$

and

$$\psi_k = Pe_z\left(\frac{H}{\varsigma_u}\varphi_k + \frac{\mathrm{d}T}{\mathrm{d}\varsigma}\right) \tag{35}$$

The exponents $s_{k1}$ and $s_{k2}$ of Eq. (33) are the roots of the characteristic equation

$$s_k^2 - Pe_z s_k - \left(Pe_z\frac{p_k}{\mu} + \frac{k_r}{k_z}\lambda_k\sigma^2\right) = 0 \tag{36}$$

The subscript $k$ has been attached to all dependent variables and factors, in order to point out that their values depend upon the separation constant $\lambda_k$.

The integration constants $\hat{c}_{k1}$ and $\hat{c}_{k2}$ of Eq. (33a) are calculated by means of the boundary conditions (24c) and (24e), leading to the system of algebraic equations

$$\begin{aligned}&\hat{c}_{k1}\left(1 - \frac{1}{Pe_z}s_{k1}\right) + \hat{c}_{k2}\left(1 - \frac{1}{Pe_z}s_{k2}\right) = \alpha_k\left(q_k(0) - \frac{1}{Pe_z}\frac{\mathrm{d}q_k(0)}{\mathrm{d}\varsigma} + \frac{H}{1+\varsigma_u Pe_z}\right)\\ &\hat{c}_{k1}s_{k1}\exp(s_{k1}) + \hat{c}_{k2}s_{k2}\exp(s_{k2}) = \alpha_k\frac{\mathrm{d}q_k(1)}{\mathrm{d}\varsigma}\end{aligned} \tag{37}$$

where from (33b) $\hat{\boldsymbol{q}}_k$ has been replaced by $-\alpha_k q_k$.

$\alpha_k$ arises in both equations as a factor of the right hand term and thus it will appear as a multiplication factor of both integration constants. Let us define

$$\begin{aligned}\hat{c}_{k1} &= \alpha_k c_{k1}\\ \hat{c}_{k2} &= \alpha_k c_{k2}\end{aligned} \tag{38}$$

inserting (38) into (33a) yields

$$\hat{\boldsymbol{h}}_k = \alpha_k h_k$$

and Eq. (33) becomes

$$Z_k = \alpha_k(h_k + q_k) \tag{39}$$

By multiplying both sides of Eq. (39) by $n/T$ and integration with respect to $\varsigma$ gives

$$n\int_0^1 \frac{Z_k}{T}\,\mathrm{d}\varsigma = \alpha_k n\int_0^1 \frac{h_k + q_k}{T}\,\mathrm{d}\varsigma \tag{40}$$

where, by definition, the left hand term is equal to $\alpha_k$. After rearranging (40), we obtain

$$\alpha_k\left[1 - n\int_0^1 \frac{h_k + q_k}{T}\,\mathrm{d}\varsigma\right] = 0 \tag{41}$$

$\alpha_k = 0$ is a trivial solution, since according to (39) $Z_k$ would be zero. The non-trivial solution of (41) requires that the term within the bracket vanishes. Condition (41) shows that both $h_k$ and $q_k$ have to be real functions and thus $p$ in (25) is a real constant.

### 2.6. Stability limits

Eq. (41) contains the basis for resolving the stability problem. For a given separation constant $\lambda_k$, (41) provides a value of $p_k$ defined in (25). If $p_k > 0$, the amplitude of a small local temperature disturbance grows exponentially with time, leading either to a dark zone and ultimately an extinction of the burner or to a temperature rise, which without any control means may lead to a damage of the catalytic panel structure. On the other hand, if $p_k < 0$, any perturbation damps out aperiodically (stable behaviour). The marginal state (neutral stability) which separates the stable from the unstable state is obtained by setting $p_k = 0$ in Eq. (41).

This equation implicitly contains $\psi$, which is defined in (35); this expression can be transformed by means of the derivative $\mathrm{d}T/\mathrm{d}\varsigma$ from (22) and the limit of Eq. (26) as $p \to 0$, thus yielding:

$$\psi = Pe_u \frac{H}{\varsigma_u^2} \exp\left(-\frac{\varsigma}{\varsigma_u}\right)\left(\frac{Pe_u}{1 + Pe_u} - \frac{\varsigma}{\varsigma_u}\right) \tag{42}$$

The solution of Eq. (41), in which (33a) and (33b) are introduced with the above expression, determines the radius of the catalytic panel corresponding to the state of neutral stability. This equation has been solved both analytically and numerically. An accurate analytical approximation for $\varsigma_u \ll 1$, is given by [1]

$$\frac{R}{z_u} \leqslant j_{1,k}\sqrt{\frac{k_r}{k_z}\frac{1}{1 + Pe_u}} \tag{43}$$

### 2.7. Numerical results

The zeros $j_{1,k}$, $k = 1, 2, 3\ldots$ of the Bessel function $J_1$ form a continuously increasing sequence of values. Setting $k = 1$ ($j_{1,1} \cong 3.832$) in (43), yields the radius of the catalytic panel for which any disturbance of the temperature distribution will either remain stationary or will be damped out aperiodically with time. The curve of neutral stability (43) is shown in Fig. 3 as a function of

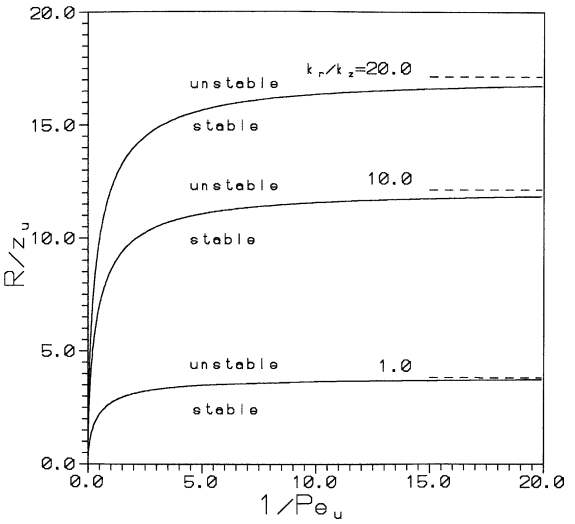


Fig. 3. Non-dimensional radius of the catalytic panel corresponding to the sate of neutral stability for various relative anisotropy of the heat conductivity.

$Pe_u^{-1}$ and $(k_r/k_z)$. The influence of an anisotropy of the thermal conductivity ($k_r/k_z > 1$) significantly increases the extent of the stable domain. Condition (43) shows also that the radius of the stable catalytic panel is proportional to the mass transfer unit length $z_u$. The latter corresponds to the $e^{-1}$ decay of the bulk concentration of the reactants and thus roughly to the thickness of the catalytic panel within which the main part of the combustion heat release takes place. According to Eqs. (12) and (13), heat production and thermal conductivity tend both to restore a stable homogeneous temperature distribution. For small $z_u$ the main part of heat production is limited to a narrow layer near the entry of the catalytic panel; thus it does not contribute significantly to restore an even temperature distribution within the rest of the panel thickness. This may explain why the maximum radius of the catalytic panel ensuring stability decreases when reducing the mass transfer unit length.

## 3. Conclusions

The purpose of the present work is to estimate the onset of an unstable temperature distribution in a plane axisymmetric catalytic burner. The instability mechanism is assumed to be related to the temperature dependence of the viscosity. Apart from the linearisation, the main underlying simplifications are (i) the assumption of equal temperature of both gas and solid at every site, (ii) the neglected radiative heat transfer, (iii) the mass transfer limited heterogeneous catalytic reaction and (iiii) the constant and steady pressure gradient across the catalytic panel. These simplifications lead to

[1] The mathematical derivation to obtain (43) is available upon request.

an analytic solution for the stability characteristics i.e., the curve of neutral stability. As the mass transfer unit length $z_u$ generally is of the order of a few mm, the stability characteristics lead to a small radius $R$ of the catalytic panel in the case of isotropic thermal conductivity. For the investigated burner (Fig. 1) and depending on the combustion parameters, $R$ for neutral stability is in the range of 1–3 cm.

However, a stable combustion behaviour can be expected for anisotropic catalytic panels with increased $R$, when the radial thermal conductivity exceeds the axial conductivity. Large relative anisotropy ($k_r/k_z = 8.8$) exists at room temperature e.g., in layered metallic fibre material [7].

The dimensional characteristics of a catalytic panel corresponding to a state of neutral stability yields a criterion to shape the catalytic panel of a combustor for avoiding the occurrence of an unstable and inhomogeneous temperature distribution. To this end, the cross-section of the combustor may be segmented into several insulated channels whose radial length scale is smaller or equal than a critical radius corresponding to the state of neutral stability. Burner with segmented catalysts already exist [10,11]. However their segmenting seemed to be motivated by thermal stress and structural reliability considerations. As another approach, Acotech company produces metal fibre burner mats which are provided with a hole pattern for stabilising the combustion reaction and to reach a homogeneous temperature distribution [12]. The appropriate distance between the holes has been determined on an experimental basis; it appears to be relatively close to the dimensional characteristics ensuring neutral stability according to (43).

The present paper is a first step to propose an explanation of the observed unstable behaviour of catalytic burners. Taking into account the numerous assumptions made, experimental and further theoretical work are required to confirm the pertinence of the proposed aerothermal instability mechanism.

## Acknowledgements

I am grateful to Prof. P. A. Monkewitz and to Dr. P. Papas, Swiss Federal Institute of Technology in Lausanne, for their comments which were very useful for reformulating some parts of this work. I want to thank my friend and colleague, J.-P. Budliger, for many discussions and useful suggestions and Dr. Mantzaras, Paul Scherrer Institute in Villigen for his very pertinent comments.

## References

[1] J.-P. Budliger, G. Capitaine, M. Chapatte, Ph. Meister, C. Mégroz, Développement d'un brûleur à combustion catalytique hétérogène, Projet NEFF no. 647, Projet FOGA no. 0027, 1997.
[2] G. Eigenberger, Mechanismen und Auswirkungen kinetischer Instabilitäten bei heterogen-katalytischen Reaktionen, Habilitationsschrift im Fachbereich Verfahrenstechnik der Universität Stuttgart, 1977.
[3] I. Yuranov, L. Kiwi-Minsker, M. Slin'ko, E. Kurkina, E.D. Tolstunova, A. Renken, Oscillatory behaviour during CO oxidation over Pd supported on glass fibers: experimental study and mathematical modeling, Chem. Eng. Sci. 55 (2000) 2827–2833.
[4] J.R. Philip, Flow in porous media, Ann. Rev. Fluid Mech. 2 (1970) 177–204.
[5] A. Schlegel, Experimentelle und numerische Untersuchung der $NO_x$-Bildung bei der katalytisch stabilisierten und der nicht-katalysierten, mageren Vormischbrennung, PhD Dissertation ETH no. 10887, Juris Druck + Verlag Dietikon, 1994.
[6] E.U. Schlünder, E. Tsotsas, Wärmeübertragung in Festbetten, durchmischten Schüttgütern und Wirbelschichten, Georg Thieme Verlag, 1988.
[7] M. Golombok, L.C. Shirvill, Laser flash thermal conductivity studies of porous metal fiber materials, J. Appl. Phys. 63 (6) (1988) 1971–1976.
[8] S. Chandrasekhar, Hydrodynamic and Hydromagnetic Stability, Dover Publications, 1981.
[9] J.P. Kesselring, Catalytic Combustion, Advanced Combustion Methods, Academic Press Inc., 1986.
[10] H. Sadamori, Application concepts and evaluation of small-scale catalytic combustors for natural gas, Catal. Today 47 (1999) 325–338.
[11] Y. Ozawa, T. Fujii, M. Sato, T. Kanazawa, H. Inoue, Development of a catalytically assisted combustor for a gas turbine, Catal. Today 47 (1999) 399–405.
[12] ACOTECH (Advanced combustion technology), Metal Fibre Burner, Surface combustion.